Article

Use of UV−vis Reflection Spectroscopy for Determining the Organization of Viologen and Viologen Tetracyanoquinodimethanide Monolayers

Pilar Cea, Santiago Martn, Ana Villares, Dietmar Mbius, and M. Carmen Lpez

More About This Article

Additional resources and features associated with this article are available within the HTML version:

- Supporting Information
- Links to the 5 articles that cite this article, as of the time of this article download
- Access to high resolution figures
- Links to articles and content related to this article
- Copyright permission to reproduce figures and/or text from this article

View the Full Text HTML

ACS Publications
High quality. High impact.

Use of UV−vis Reflection Spectroscopy for Determining the Organization of Viologen and Viologen Tetracyanoquinodimethanide Monolayers

Pilar Cea,[†] **Santiago Martín,**[†] **Ana Villares,**[†] **Dietmar Möbius,**[‡] **and M. Carmen López*,**[†]

Departamento de Química Orgánica-Química Física, Facultad de Ciencias, Plaza de San Francisco, Ciudad Universitaria, 50009 Zaragoza, Spain, and Max Planck Institute for Biophysical Chemistry Am Fassberg 11, 37077 Göttingen, Germany

UV−vis reflection spectroscopy has been used for proving in situ the organization of pure viologen and hybrid viologen tetracyanoquinodimethanide monolayers at the air−water interface. Other more classical measurements concerning Langmuir monolayers, including surface pressure−area and surface potential−area isotherms, are also provided. The organization of the viologen in the Langmuir monolayer was investigated upon the different states of compression, and the tilt angle of the viologen moieties with respect to the water surface was determined. A gradual transition of the viologen molecules from a flat orientation in the gas phase to a more tilted position with respect to the water surface in the condensed phases occurs. The addition of a tetracyanoquinodimethane (TCNQ) salt in the subphase leads to the penetration of TCNQ anions into the positively charged viologen monolayer forming a hybrid viologen tetracyanoquinodimethanide film where a charge-transfer interaction between the two moieties is observed. From a quantitative analysis of the reflection spectra, an organization model of these hybrid monolayers at the air−water interface is proposed, suggesting a parallel arrangement of viologen and TCNQ units with a 1:2 stoichiometry.

Introduction

Monomolecular films at the air−water interface have gained the attention of many research groups in the last two decades due to both their theoretical interest and their potential use in the development of components for industrial applications. The reason for such an interest lies in the molecular architecture achieved by these monolayers that confers properties upon them that can be very different from those of unoriented bulk materials. Nevertheless, the prerequisite to the final application of these organized systems is an extensive knowledge of the structure of the monolayer itself, i.e., a thorough understanding of the monolayer behavior is essential for exploiting the technique of Langmuir and Langmuir−Blodgett (LB), which allows the creation of films with a high internal order, the desired number of layers, and the possibility of depositing alternate monolayers of different molecules. In this context, researchers around the world have developed a number of surface-sensitive experimental methods for proving "in situ" the organization of molecules on the water surface.[1] One of these techniques is UV−vis reflection spectroscopy[2,3] whose main advantage is that it applies to the air−water interface, affording an "in situ" study of the monolayer and detection of physical or chemical processes such as adsorption or penetration of molecules from the solution into the interface (the bulk subphase is not recorded by this method) or polymerization reactions at the interface;[4] it also provides information about the aggregation state of the molecules,[5] the formation of hydrogen bonds,[6] or, by means of the appropriate calculations, the determination of the tilt angle of the molecules at the air−water interface.[3,7]

Some of the most fascinating electrochemical compounds studied in Langmuir and Langmuir−Blodgett films are viologens

or salts of 4,4′-bipyridine. The electrochemical properties of LB films of viologens have shown a great dependence on several parameters including the orientation of the molecules on the films[8−13] as well as the type of counterion[14−17] present in the subphase and, therefore, incorporated into the LB film during the transference process.[18] Although there is a considerable body of published work dealing with the electrochemistry of thin solid films of viologen derivatives[8−10,16,17,19−24] as well as other potential applications of these viologen films,[25−27] there is relatively little data available for the detailed organization of amphiphilic viologens at the air−water interface.[28] Therefore, one of the aims of this paper is to discuss the "in situ" characterization of Langmuir films of a viologen derivative (structure shown in Chart 1a) onto pure water by means of UV−vis reflection spectroscopy in addition to complementary data provided by the usual monolayer techniques.

On the other hand, electrically active LB films based on charge transfer (CT) complexes have attracted a lot of attention for application in nanoscale molecular devices including electrical circuits, rectifiers, nanowires, switches, and sensors. It has been reported elsewhere that tetracyanoquinodimethanide counterions strongly affect the electrochemical properties of viologens in the solid state and solutions[29−34] as well as in LB films.[16,17] Thus, in this paper we also try to provide some insight about the organization of hybrid viologen tetracyanoquinodimethanide films that were fabricated spreading the viologen onto aqueous solutions containing a tetracyanoquinodimethane (TCNQ) salt (Chart 1b). It is well-known that viologens and tetracyanoquinodimethanide anions form CT complexes in the solid state[30] characterized by a broad and relatively intense band in the UV−vis region. Consequently, the formation of a CT complex when a viologen derivative is spread onto an aqueous subphase containing a tetracyanoquinodimethanide salt is likely and probably detectable by means of the reflection spectroscopy. Moreover, the use of aqueous solutions of LiTCNQ as subphase

* Corresponding author. E-mail address: mcarmen@unizar.es. Telephone number: 00 34 976 76 22 96. Fax number: 00 34 976 76 12 02.
† Ciudad Universitaria.
‡ Max Planck Institute for Biophysical Chemistry.

CHART 1: Chemical Structures of (a) 1,1′-Dioctadecyl-4,4′-bipyridilium Dication and (b) Tetracyanoquinodimethanide Anion

$C_{18}H_{37}$–N^+ ⬡ ⬡ N^+–$C_{18}H_{37}$

a

(NC, NC)C=⬡=C(CN, CN) $^{\cdot-}$

b
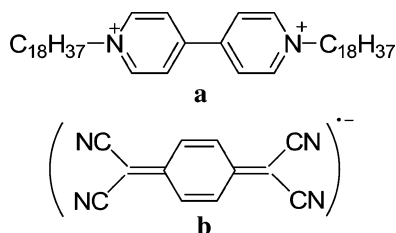
has certain advantages from the point of view of the Langmuir film characterization. Thus, the LiTCNQ–water solutions have a band in the visible region (around 600 nm), far from that due to the viologen moiety (around 270 nm), and therefore, the TCNQ moieties should be easily detected by reflection spectroscopy if they penetrate into the floating monolayer providing information about the interactions between the viologen and the TCNQ$^{\cdot-}$ as well as data about the orientation of the anions in the monolayer. Furthermore, some models about the arrangement of the viologens in the monolayer at the air–water interface as well as the penetration of the TCNQ anions onto the monolayer and their relative orientation with respect to the viologen moieties are presented.

Experimental Section

1,1′-Dioctadecyl-4,4′-bipyridilium dibromide, $(2C_{18}V)Br_2$, and 1,1′-dimethyl-4,4′-bipyridilium dichloride (methyl viologen) were purchased from Aldrich, and no further treatment was carried out. Solutions of $(2C_{18}V)Br_2$ were prepared in chloroform/absolute ethanol in the rate 4:1. The chloroform was HPLC grade (99.9%) purchased from Aldrich, and the ethanol was HPLC grade (99.0%) purchased from Normasolv. The solutions were used as fresh as possible. Li(TCNQ) was provided by Dr. Ballester from Universidad Complutense de Madrid (Spain). Its purity (better than 99.0%) was checked by spectroscopic techniques. Aqueous solutions of LiTCNQ to be used as subphase in the trough experiments were prepared employing Millipore Milli-Q water whose resistivity was 18.2 MΩ·cm. The LiTCNQ solutions were stored in darkness, and they were always used within 1 month.

The films were prepared on a NIMA trough whose dimensions are 720 × 100 mm^2. Floating monolayers or Langmuir films were fabricated spreading 0.5 mL of a 10^{-4} M solution of $(2C_{18}V)Br_2$ onto water or aqueous solutions of LiTCNQ 10^{-6} or 2 × 10^{-6} M. The spreading solution was delivered from a syringe held very close to the surface allowing the surface pressure to return to a value as close as possible to zero. The initial surface density of the films was such that the surface pressure never exceeded 1 mN/m. The monolayer compression started after waiting for 15 min so that the solvent had completely evaporated, and it was carried out at a constant sweeping speed of 6.6 × 10^{-3} nm^2/(molecules·min). Each compression isotherm was registered at least three times to ensure the reproducibility of the obtained results. All the experiments were performed in a clean room whose temperature was kept constant at 20 ± 1 °C. The ΔV–A measurements were carried out with a vibrating plate condensor of the type described earlier.[35] As counter electrode, a squared Pt plate 3 cm in length was placed at the bottom of the trough. The UV–vis reflection experiments, whose fundamentals were reported elsewhere,[2] were recorded with a spectrophotometer provided by Nanofilm Technologie GmbH. The reflection spectrometer has a light
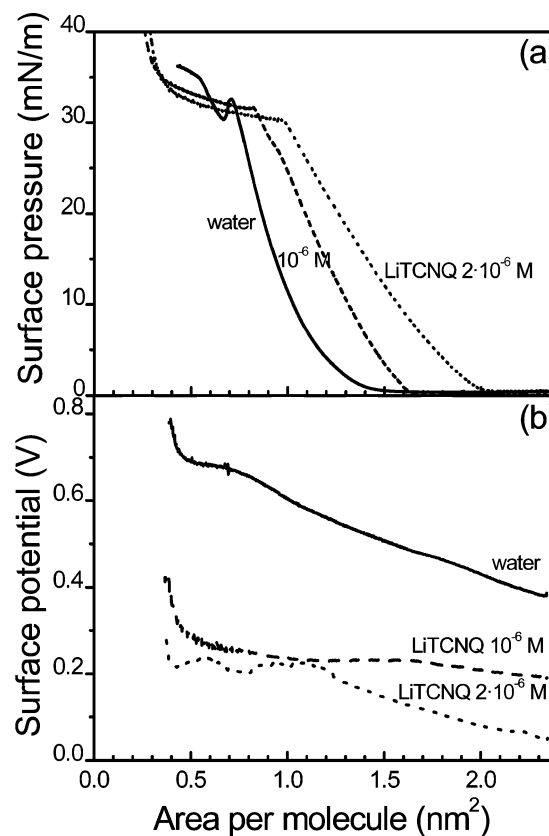

Figure 1. (a) Surface pressure and (b) surface potential vs area per $C_{18}V$ molecule isotherms onto the indicated subphases.

source FiberLight DTM 6/50 which consists of a deuterium lamp and a tungsten lamp which are both installed in a ceramic cell. An internal lamp shutter is electronically controlled. The FiberLight produces white light in the spectral range from 240 to 1000 nm, and there is a multichanel spectrometer for analyses in the same spectral range using a grating and a CCD diode array as detector. The absolute wavelength accuracy is <0.3 nm; the resolution (Rayleigh-criterion) is >3 nm. A bifurcated UV–vis fiber with 20 multimode fibers in each arm conducts, through the first arm, the light from the source to a sensor unit that collimates the light to the monolayer and focuses the reflected light into the fibers that, through the second fiber arm, is conducted to the spectrometer. A blackplate situated in the bottom of the trough is used to eliminate the stray light. The background correction spectrum (clean surface) is taken prior to the spreading process. The software provided by Nanofilm and Nima permits control of the trough and the reflection spectrometer recording the π–A isotherms and reflection spectra simultaneously. The low barrier speed was chosen to minimize the relaxation phenomena of the monolayer during the recording of the reflection spectra.

Results and Discussion

The surface pressure/area per molecule (π–A) isotherms for the viologen derivative together with the surface potential (ΔV–A) isotherms are shown in parts a and b of Figure 1, respectively, for the following subphases: (i) pure water, (ii) 10^{-6} M, and (iii) 2 × 10^{-6} M aqueous solutions of LiTCNQ.

When the subphase is pure water, the surface pressure starts rising at an area of ca. 1.50 nm^2/molecule. Meanwhile, the take off in the isotherm takes place at a higher area, ca. 1.65 nm^2/molecule, if a 10^{-6} M LiTCNQ aqueous solution is employed as subphase, and at 2.05 nm^2/molecule when the subphase is

Determining Monolayer Organization

J. Phys. Chem. B, Vol. 110, No. 2, 2006 **965**
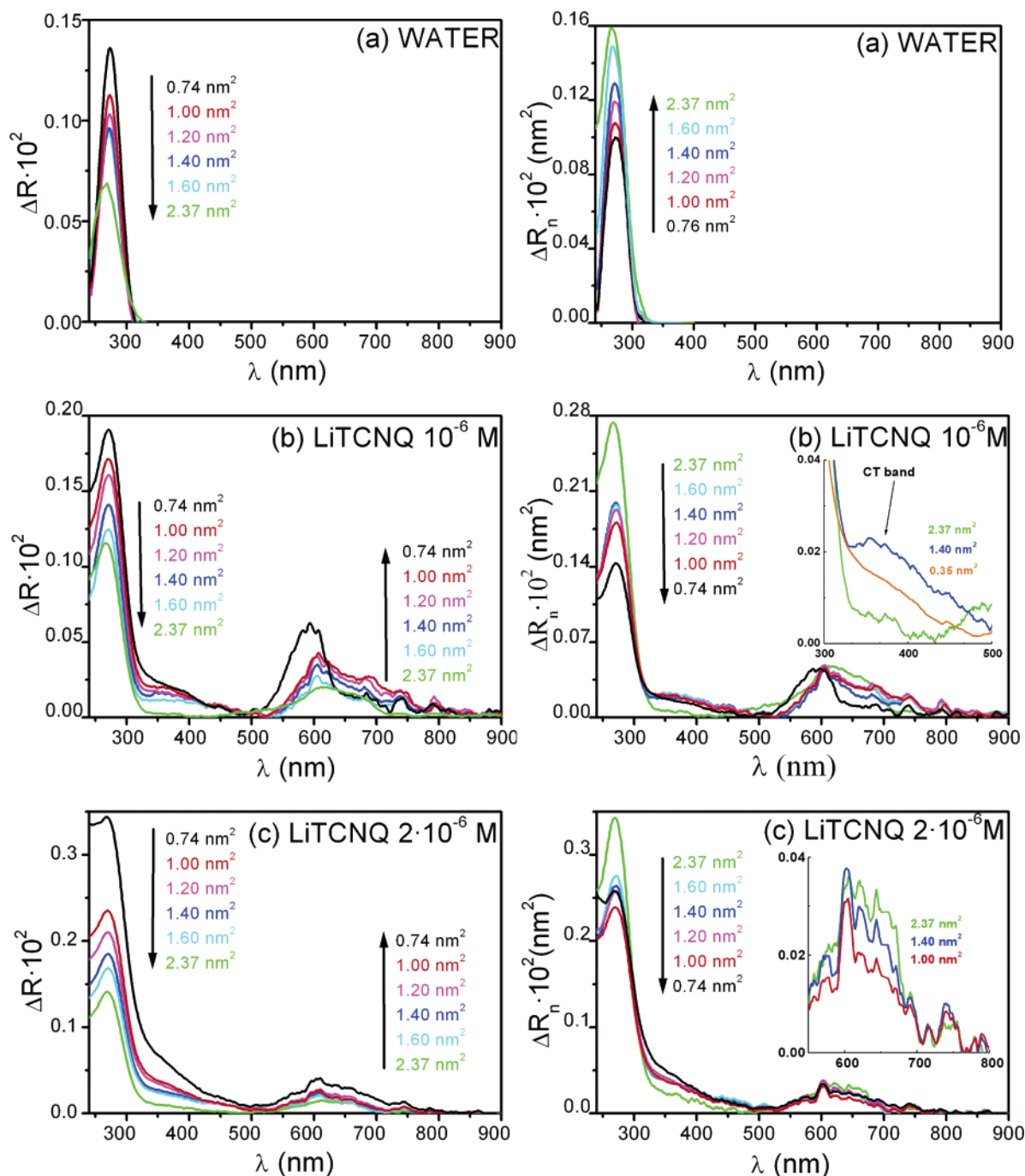
Figure 2. Reflection spectra (left) and normalized reflection spectra (right) of viologen monolayers spread onto the indicated subphases. The inset graphs are magnifications of certain regions of interest discussed in the text.

2×10^{-6} M LiTCNQ. The surface pressure increases monotonically upon compression until an overshoot above 30 mN/m is reached when the subphase is pure water. When the subphase contains the TCNQ salt, the overshoot is less evident although a drastic change in the slope of the isotherm can also be seen.

The precise surface pressure, shape, and size of the overshoot are highly dependent on the sweeping speed and on the subphase nature. The size and shape of the plateau region after the overshoot also depend on the subphase nature as can be seen in Figure 1a as well as on the speed of compression (data not shown although a comparison can be made with previously reported data[10,16]). The presence of overshoots in $\pi-A$ isotherms has been widely reported by many authors and attributed to several reasons including (i) slow rearrangement of the headgroups,[36] (ii) a change in steric configurations,[37] (iii) a lack of

nucleation for the formation of domains during the nonequilibrium compression process,[38] or (iv) collapse of the monolayer.[39] Such a phenomenon has also been observed in isotherms of viologen derivatives using subphases different from those reported here.[18,19] Nevertheless, no definite cause of the overshoot in $\pi-A$ isotherms of viologen derivatives has been reported although some authors[10,16,18,19] have indicated that it could be due to either a bilayer formation or a reorganization of the viologen units from a horizontal position to a more vertical one. In any case, it is difficult to establish the origin of the overshoot and the plateau of the isotherm just from the isotherms.

The expansion of the viologen monolayer when the TCNQ salt is added to the subphase could be due to either (i) the incorporation of the organic anion into the viologen monolayer

separating these molecules laterally or (ii) the TCNQ arranged underneath the viologen pulling the viologen molecules apart. The first explanation seems more reasonable according to the experimental data provided both by the $\Delta V-A$ isotherms and by the reflection spectroscopy data that are shown below. The surface potential of the monolayer decreases considerably when the subphase is a LiTCNQ solution compared to a pure water subphase. However, the obtained value cannot be explained just by modifying the electric double layer due to adsorption of the TCNQ$^{\bullet-}$ underneath the viologen as shown below. The monolayer surface potential, ΔV, when the double layer contribution (ionized monolayers), Ψ_0, is included in the Helmholtz equation,[40] is given by[1]

$$\Delta V = (\mu_n/A\epsilon_r\epsilon_0) + \Psi_0 \qquad (1)$$

where μ_n is the normal component of the dipole moment per molecule and ϵ_r and ϵ_0 are the relative water dielectric constant and the permittivity of the vacuum, respectively. Ψ_0 can be obtained from the Gouy−Chapman model. Thus, if the surface is supposed to be uniformly charged, homogeneous, and considered as a nonpermeable plane, and assuming that the double layer consists of single point charges, then the Gouy−Chapman model leads to the equation[41−43]

$$\Psi_0 = \frac{2kT}{e}\sinh^{-1}\left(\frac{e\alpha}{A\sqrt{8\epsilon_r\epsilon_0 kTC_b}}\right) \qquad (2)$$

where k is Boltzmann's constant, T is the absolute temperature, e is the electron charge, α is the degree of dissociation of the headgroup, A is the area per molecule, and C_b is the bulk counterion concentration in the subphase (the counterions of the positively ionized viologen monolayers are OH$^-$ and TCNQ$^{\bullet-}$ when pure water [10] and LiTCNQ solution[16] are used as subphases, respectively).

When the pure viologen monolayer is formed onto a pure water surface, the experimental surface potential at 1 nm^2/molecule is around 0.675 V, while it drops down to 0.233 and 0.219 V for the monolayer spread onto an aqueous solution of 10^{-6} M and 2×10^{-6} M LiTCNQ, respectively. Therefore, the change in surface potential at 1 nm^2/molecule is 0.442 V (10^{-6} M LiTCNQ) and 0.456 V (2×10^{-6} M LiTCNQ) with respect to the pure water subphase. Nevertheless, according to eqs 1 and 2, if the surface density of the adsorbed ions is not more than that of the headgroups, the drop surface potential should be around 0.060 and 0.075 V for 10^{-6} M LiTCNQ and 2×10^{-6} M LiTCNQ, respectively. The differences between the experimental values and those obtained from the Gouy−Chapman model could be due to the incorporation of the TCNQ anion inside the viologen monolayer,[44] resulting in the formation of one more double electric layer inside the monolayer. This layer consists of positively charged viologen groups and negatively charged TCNQ ions. The latter have a negative contribution to the total potential, explaining the low surface potential of the monolayers spread onto the LiTCNQ solutions.

The expansion of the isotherms and the drastic drop in surface potential when LiTCNQ is present in the subphase point out the incorporation of the TCNQ anions into the monolayer, but this phenomenon is more clearly evidenced by reflection spectroscopy at the air−water interface. Reflection spectra, ΔR, of monolayers on a water subphase at several surface pressures are shown in Figure 2a as well as the normalized reflection spectra defined as $\Delta R_n = \Delta R \cdot$area per molecule. Parts b and c of Figure 2 show the spectra of monolayers prepared onto 10^{-6} and 2×10^{-6} M LiTCNQ subphases, respectively. The broad
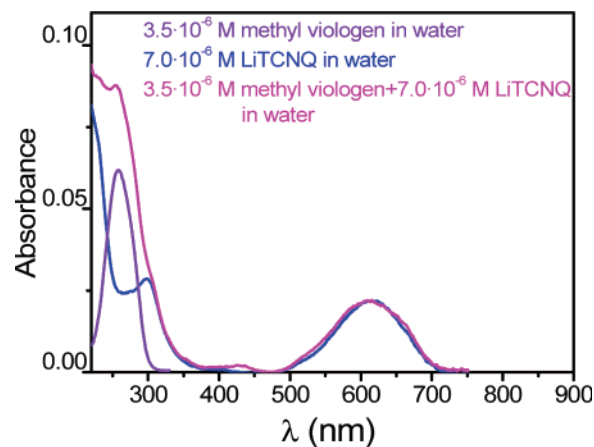
Figure 3. UV−vis spectra of pure methyl viologen and pure LiTCNQ solutions in water together with their mixture in the 1:2 proportion (cuvette length = 1 cm).
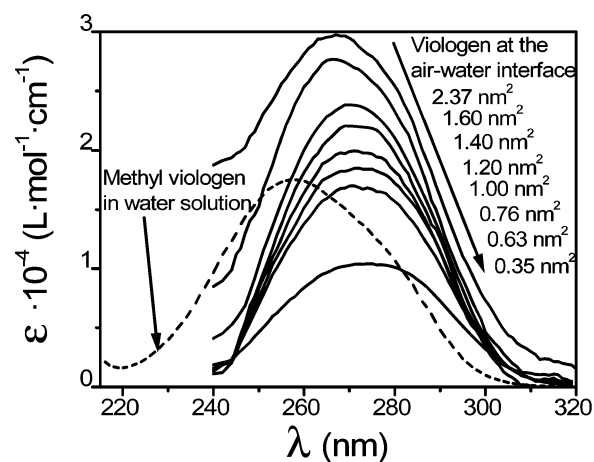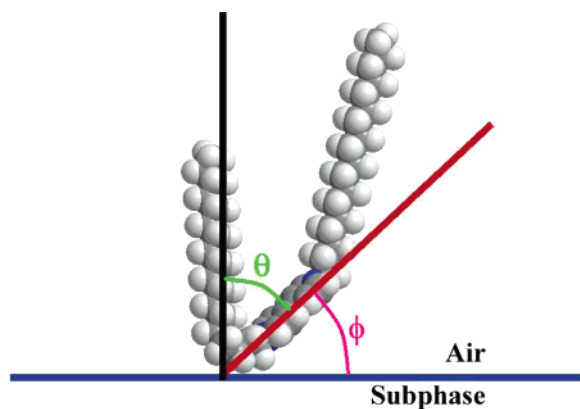

Figure 4. Molar absorptivity of a viologen monolayer onto a water subphase recorded at several surface densities and molar absorptivity of methyl viologen in water solution.

band in the 600−700 nm region, attributable to the TCNQ anions in a dimeric state, indicates the presence of TCNQ anions at the air−water interface. Obviously, such a band is not present when pure water is employed as subphase. Moreover, there is another broad band situated in the 300−450 nm region. Typically, a charge transfer (CT) complex is detected in the UV−vis range when two compounds are brought together and a new band is formed that was not present in the spectrum of either component (see Figure 3). Viologens are excellent electron acceptors and TCNQ$^{\bullet-}$ is a well-known donor which makes highly probable a CT interaction between the two components. The appearance of a band in this region of the spectrum has been previously attributed to a CT interaction in viologen derivatives,[29,45] and some authors reported the formation of viologen−TCNQ charge-transfer complexes in the solid state.[29] So far, there are no reliable accounts of solution phase CT of viologens with TCNQ,[29] although a tiny new band at ca. 420 nm can be seen in a water solution containing the two materials (Figure 3).

Figure 4 shows the comparison between the molar absorptivity spectra of the 1,1′-dioctadecyl-4,4′-bipyridilium cation at the air−water interface at several surface pressures and the spectrum of methyl viologen dichloride in water. This last compound was chosen for this comparison instead of 1′-dioctadecyl-4,4′-bipyridilium dibromide given that the methyl viologen is water soluble and therefore the environment in a water solution resembles more the one at the air−water interface

Determining Monolayer Organization

J. Phys. Chem. B, Vol. 110, No. 2, 2006 **967**

CHART 2: Definition of the θ Angle (angle between the normal to the surface and the transition moment of the viologen moiety) and its Complementary Angle ϕ

Figure 5. $\pi-A$ isotherm of the viologen derivative onto a pure water subphase (left) and tilt angle formed by the dipole transition moment of the viologen and the water surface (right) vs area per molecule.

instead of an organic solvent. The molar absorptivity (ϵ) vs wavelength spectra shown in Figure 4 have been calculated according to the following:

air−water interface[2]

$$\epsilon = \Delta R/2.303\Gamma 10^{-3}R_{\mathrm{w}}^{1/2} \qquad (3)$$

solution

$$\epsilon = A/Cl \qquad (4)$$

where Γ is the surface density given in mol·cm^{-2}, R_{w} is the water reflectivity, A is the absorbance, C is the solution concentration, and l is the cell width. C and l units are mol·L^{-1} and cm, respectively. Therefore, ϵ is expressed in cm^{-1}·mol^{-1}·L.

As can be seen in Figure 4, there is a red shift of the maximum wavelength of the spectra recorded at the air−water interface compared to the solution spectrum. This red shift could be attributed to either the formation of associates of the viologen units or, more likely, taking into account that we are dealing with a small shift, to a less polar environment. This less polar environment of the viologen moiety could be due to the contact of the chromophore unit with at least one hydrocarbon chain when the surface pressure increases, which would indicate an increase in the tilt angle when the area per molecule decreases. We will see shortly that a quantitative analysis of these spectra confirms an increase in the tilt angle of the viologen unit with respect to the water surface upon compression.

In solution, the orientation of the viologen units is at random and, therefore, the absorption must be proportional to a factor of $^2/_3$ given that only two out of the three components of the transition moment of the viologen group are interacting with the incident unpolarized light.[7] Nevertheless, at the air−water interface, there is a preferential orientation of the viologen units which, according to Figure 4, must change under compression, i.e., the more parallel the transition moment of the viologen to the water surface the higher the intensity of the reflection spectrum; therefore, an orientation factor can be defined.[7] For a general case, and with a statistical distribution of the transition moments around the surface normal, the orientation factor is given by

$$f_{\mathrm{orient}} = \frac{3}{2}\sin^2\theta \qquad (5)$$

where θ is the angle formed by the normal to the surface and the transition dipole moment of the viologen unit (Chart 2).
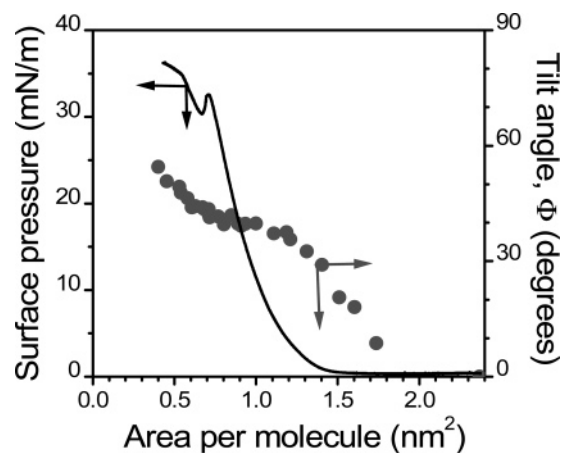
This equation is applicable only if there is a homogeneous distribution of the viologen transition moments around the surface normal. In conclusion, the decrease in the normalized spectrum when the surface pressure increases is related to an increase in the tilt angle of the viologen moiety with respect to the water surface. In the lines below, the calculation to obtain this tilt angle is presented.

An integration of the absorption band of the methyl viologen in water yields an oscillator strength of $f = 0.5028$ according to the equation[46]

$$f = \frac{4\epsilon_0 2.303 m_{\mathrm{e}}c_0}{N_{\mathrm{A}}e^2}\int_{\mathrm{band}}\epsilon\,\mathrm{d}\upsilon = 1.44\times10^{-19}\int_{\mathrm{band}}\epsilon\,\mathrm{d}\upsilon \quad (6)$$

where ϵ_0 is the permittivity of vacuum, m_{e} the electron mass, e the electron charge, c_0 the light speed in a vacuum, and N_{A} the Avogadro constant. The factor 1.44×10^{-19} is expressed in mol·L^{-1}·cm·s. The value of the oscillator strength of $(2C_{18}V)$-Br$_2$ has been determined in acetonitrile yielding a value of 0.5169, which is quite similar to that of methyl viologen in water. We have chosen the oscillator strength of methyl viologen in water for the calculations in order to minimize the possible effect of the solvent.[47]

The comparison of the oscillator strength obtained in solution with the apparent oscillator strength, f_{app}, calculated from the measured reflection spectra, allows the determination of the orientation factor defined as

$$f_{\mathrm{orient}} = \frac{f_{\mathrm{app}}}{f} \qquad (7)$$

where f_{app} is given by[7]

$$f_{\mathrm{app}} = 2.6\times10^{-12}\int_{\mathrm{band}}\mathrm{area}\,\Delta R\,\mathrm{d}\upsilon =$$
$$2.6\times10^{-12}\int_{\mathrm{band}}\Delta R_{\mathrm{n}}\,\mathrm{d}\upsilon \quad (8)$$

The numeric factor 2.6×10^{-12} is expressed in nm^{-2}·s. Substitution of the values obtained in eq 6 (oscillator strength) and eq 8 (apparent oscillator strength) in eq 8 give the orientation factor that substitution in eq 5 yields the angle, θ, formed by the normal to the surface and the dipole transition moment of the viologen unit.

Figure 5 shows the $\pi-A$ isotherm (left) together with the tilt angle, ϕ (right), defined as the tilt angle with respect to the water surface ($\phi = 90 - \theta$) expressed in degrees (see Chart 2),

vs the area per molecule. It should be noted that spectra recorded in the gas phase of the isotherm ($2.37-1.50$ nm^2) show a high dispersion in the angle values, probably due to the presence of nonuniform domains in the monolayer underneath the fiber-optics detector, that produce significant fluctuations in the signal[48] from one measurement to another. As soon as the isotherm takes off, all the spectra follow a logical evolution and the three experiments performed yielded very reproducible tilt angle values. From Figure 5 it can be concluded that, at low surface density, the viologens are situated in a lying flat position (more polar environment and shorter value of the maximum absorption wavelength), but as the surface pressure increases, the viologen units suffer a transition to a more vertical position (less polar environment of the viologen units and slight red shift of the maximum wavelength). There are two sudden changes in the tilt angle of the viologen groups upon compression, the first one takes place between 2 and 1.5 nm^2, i.e., in the region prior to the increase in the surface pressure, and the second one occurs in the vicinity of the overshoot in the isotherm. Before the overshoot, the aromatic rings of the viologen derivative have a tilt angle of ca. 43° with respect to the water surface; afterward, in the region after the overshoot, ϕ gradually increases until it reaches ca. 50°, indicating that the overshoot is caused by a reorganization of the viologen units but not a collapse, where a drastic increase in the reflection intensity due to a multilayer formation would have been expected and, therefore, an apparent decrease in the tilt angle of the viologen group. Such an increase in the intensity of the reflection spectra is effectively observed in the collapse of the monolayer (spectra not shown for clarifying purposes). A complete description of the overshoot should also take into consideration other factors. Thus, as we said above there is a significant influence of the speed of compression on the size of the overshoot and the precise surface pressure at which it appears; this indicates a kinetic factor that has been previously interpreted[49] as metastability of the monolayer in this region. The alkyl chains have been reported[50] to play an important role on the surface pressure of the plateau in the isotherms giving that lateral side chain interactions contribute significantly to monolayer stability. The absence of a constant surface pressure plateau as observed here has also been related to side chain crystallization by Xiao et al.[51] Data provided by other techniques, capable of analyzing the alkyl chain behavior upon the monolayer compression, could contribute to complete the information provided by the reflection spectroscopy.

A similar procedure can be applied to calculate the tilt angle of the viologen unit and even the tetracyanoquinodimethanide anions when a LiTCNQ aqueous subphase is employed. Nevertheless, these calculations present certain difficulties. Thus, there are three unknown quantities ($\theta_{viologen}$, θ_{TCNQ}, and the average number of TCNQ anions incorporated per viologen unit), but there are only two bands to be integrated; i.e., we have a system of two equations and three unknown quantities. Besides, it should be taken into account that TCNQ$^{\bullet-}$ moieties present a band in the $240-320$ nm region that overlaps the viologen band. Therefore, the band observed in the reflection spectra is the contribution of the viologen and the TCNQ$^{\bullet-}$. Consequently, we should discriminate between these two contributions in order to calculate the tilt angle of both materials. To do so, we have assumed that the more stable situation in the monolayer should correspond to a parallel arrangement of the viologen units and the TCNQ anions. In this way, the interaction of the two aromatic units would be maximum with a better charge compensation and a more effective interaction
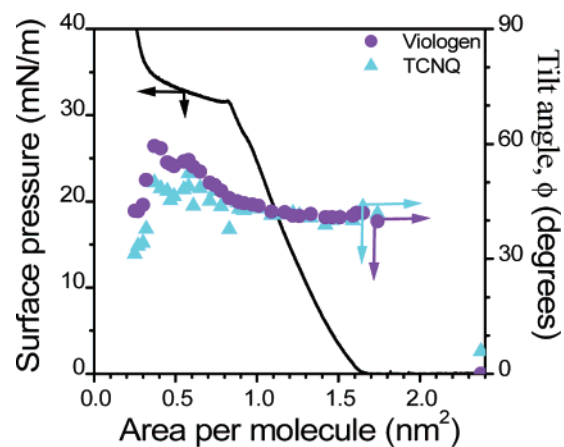
Figure 6. $\pi-A$ isotherm of the viologen derivative onto a 10^{-6} M LiTCNQ aqueous subphase (left) and tilt angle formed by the transition moment of the viologen (circles) or TCNQ (triangles) and the liquid surface (right) vs area per molecule. The tilt angles have been calculated assuming a viologen/TCNQ 1:2 stoichiometry.

CHART 3: Model of Organization of Viologen Tetracyanoquinodimethanide Monolayers at the Air−Water Interface
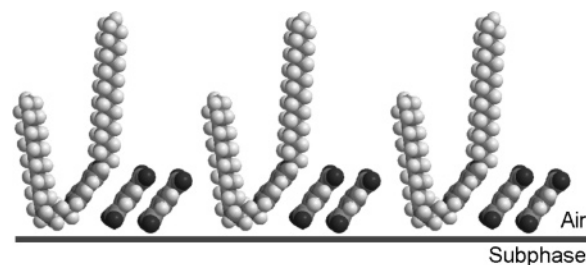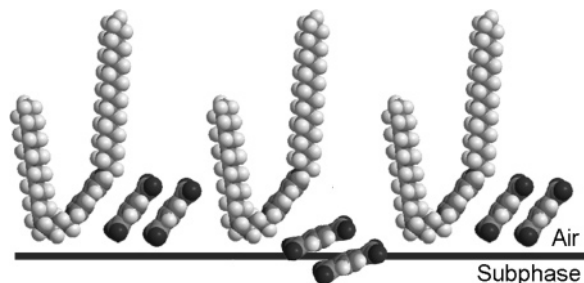

to form the CT complex. Therefore, the TCNQ moieties should have a very similar tilt angle to that of the viologen. The tilt angle of the TCNQ anions can be easily determined by means of the integration of the $500-800$ nm band in the reflection spectra, taking into account the number of TCNQ anions incorporated per viologen unit, and the calculation of the oscillator strength from solution ($f = 0.0357$). On the other hand, the oscillator strength corresponding to the $240-320$ nm band has been estimated as the sum of the viologen oscillator strength ($f = 0.5028$) and the TCNQ$^{\bullet-}$ oscillator strength ($f = 0.2553$) multiplied by the number of TCNQ anions incorporated into the monolayer. If ϕ values obtained from the integration of the bands in the $240-320$ nm and $500-800$ nm coincide or are very similar to each other, the hypothesis of a parallel arrangement of the two moieties would be plausible. These calculations have been performed for several viologen/TCNQ stoichiometries obtaining significant differences between the tilt angle calculated from the integration of the two bands, except in the case of a viologen/TCNQ 1:2 stoichiometry where an excellent agreement is obtained before the overshoot as shown in Figure 6 for a LiTCNQ 10^{-6} M subphase (the same stoichiometry is obtained for a LiTCNQ 2×10^{-6} M subphase as we will see later on). Besides, the last situation would be stoichiometry of charges. On the basis of these results, a schematic model of molecular organization at the air−water interface is depicted in Chart 3.

The excellent agreement between the viologen and the TCNQ$^{\bullet-}$ tilt angle in the region between the gas phase and the overshoot is not accomplished after the overshoot. The apparent tilt angle of the TCNQ$^{\bullet-}$ is lower than that obtained for the viologen indicating that the intensity of the TCNQ$^{\bullet-}$ spectrum is higher than expected for a parallel arrangement of the viologen

Determining Monolayer Organization

J. Phys. Chem. B, Vol. 110, No. 2, 2006 **969**

CHART 4: Model of Organization of Viologen Tetracyanoquinodimethanide Monolayers at the Air−Water Interface after the Overshoot

Figure 7. $\pi-A$ isotherm of the viologen derivative onto a 2×10^{-6} M LiTCNQ aqueous subphase (left) and tilt angle formed by the transition moment of the viologen (circles) or TCNQ (triangles) and the liquid surface (right) vs area per molecule. The tilt angles have been calculated assuming a viologen/TCNQ 1:2 stoichiometry.

and TCNQ$^{•−}$ for a 1:2 stoichiometry; i.e., the model proposed in Chart 3 is no longer valid beyond the overshoot. We have thought about two possible explanations for this discrepancy. The first proposal is a sudden incorporation of more TCNQ units into the monolayer which would cause an increase in the intensity of the band around 600 nm. This hypothesis could agree with the formation of H aggregates (blue shift of the TCNQ-band). Nevertheless, we do not give much credibility to this model as a decrease in the ΔV values would be expected and, on the other hand, it is hard to believe that in a compact state of the monolayer more anions are incorporated, especially if the viologen charge was already compensated before the overshoot. The second possibility is that a small number of TCNQ anions are expelled from their initial position in the monolayer, due to steric hindrance at a high compression state of the monolayer, and these anions are situated underneath the viologens acquiring a lower tilt angle with respect to the water surface, justifying in this way a more intense band in the reflection spectra (perhaps forming H aggregates with other TCNQ anions in the subphase) and a worse viologen charge compensation according to an abrupt increase in the surface potential as observed in Figure 1. The CT band intensity in the normalized reflection spectra increases its intensity when the surface density increases (inset Figure 2b right) suggesting a more effective CT interaction between the viologen and the TCNQ units, probably favored by a more compact packing when the surface pressure increases. Nevertheless, after the overshoot this tendency (increase of the CT band) is inverted indicating that now there is a worse CT interaction, which supports this second proposal. Chart 4 illustrates this model.

The spectra recorded on a 2×10^{-6} M LiTCNQ subphase were analyzed in the same way as for the 10^{-6} M LiTCNQ subphase. Again the agreement between the viologen and TCNQ$^{•−}$ tilt angles is achieved for a 1:2 stoichiometry before the plateau in the isotherm (Figure 7). The main difference between the results obtained in both subphases is the different tilt angle, being lower when a more concentrated subphase is employed. Probably, a higher TCNQ$^{•−}$ concentration yields a less polar environment at the air−water interface and, therefore, the viologen units tend to increase their contact surface with the aqueous surface. A lower tilt angle is in agreement with the expansion of the monolayer when the LiTCNQ concentration increases. On the other hand, after the beginning of the plateau in the isotherm, the angles obtained for the viologen and the TCNQ$^{•−}$ are different, indicating that either the stoichiometry proportion changes or the assumption that the viologen and TCNQ anions are parallel to each other is no longer true. In this case, unlike the less concentrated LiTCNQ solution, the discrepancy occurs not immediately after the overshoot but a bit later. The reason the model proposed in Chart 3 is not valid at high surface densities in the plateau region could be in this
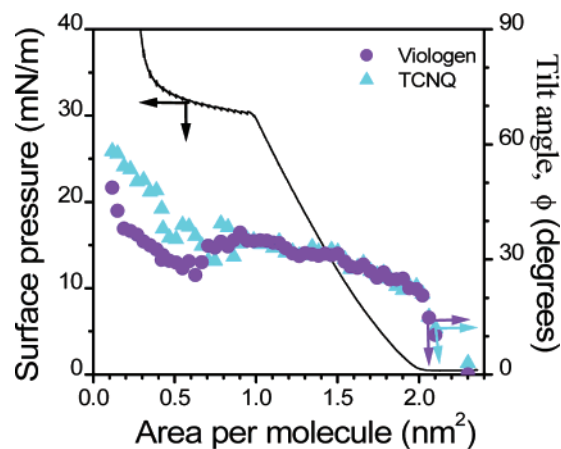
case an ejection of some TCNQ anions from the interface to the subphase where they are not recorded by reflection spectroscopy. Thus, if we assume that the TCNQ anions in the interface are still parallel to the viologen ones in the plateau region, a 1:1 stoichiometry is needed to reach an agreement between both angles, which means that some TCNQ anions have gone into the subphase, which is in agreement with the increase of the surface potential observed in Figure 1.

Conclusions

This paper has aimed at a better understanding of the organization of viologen monolayers at the air−water interface. The $\pi-A$ and $\Delta V-A$ isotherms as well as reflection spectroscopy indicate that viologen moieties undergo a gradual transition from a more or less flat orientation in the gas phase to a tilted one, showing an angle of ca. 43° before the overshoot. The overshoot in the $\pi-A$ isotherm has been interpreted as a further reorganization of the molecules at the air−water interface, reaching a tilt angle above 50° after the plateau in the isotherm. Other factors such as kinetic effects and influence of alkyl chains could also play a significant role on the overshoot.

Researchers worldwide have always sought fruitful combinations of molecules to produce new complexes, adducts, or compounds showing new and useful properties. Thus, prompted by these attempts we have prepared hybrid viologen tetracyanoquinodimethanide monolayers at the air−water interface by means of the incorporation of TCNQ anions from the subphase into the positively charged viologen monolayers. Such a penetration of the subphase anions into the monolayer was demonstrated by means of the $\pi-A$, $\Delta V-A$, and more clearly by UV−vis reflection spectroscopy. A simultaneous quantitative analysis of the two active molecules in the UV−vis region has facilitated the investigation of the viologen tetracyanoquinodimethanide hybrid monolayers allowing the suggestion of an organization model at the air−water interface. In this model, a parallel arrangement of viologen and TCNQ units with a 1:2 stoichiometry is proposed. After the overshoot this model is no longer valid and a possible explanation is that TCNQ units are ejected from their initial position in the monolayer, being just adsorbed beneath the viologen units in a more horizontal position or even squeezed into the subphase. Throughout this paper UV−vis reflection spectroscopy has shown itself as a powerful tool for the in situ characterization of floating monolayers from a

Cea et al.

qualitative and a quantitative point of view, allowing the determination of the penetration rate of materials present in the subphase into the monolayer.

References and Notes

(1) Dynarowicz-Latka, P.; Dhanabalan, A.; Oliveira, O. N., Jr. *Adv. Colloid Interface Sci.* **2001**, *91*, 221.

(2) Grüniger, H.; Möbius, D.; Meyer, H. *J. Chem. Phys.* **1983**, *79*, 3701.

(3) Orrit, M.; Möbius, D.; Lehmann, U.; Meyer, H. *J. Chem. Phys.* **1986**, 4966.

(4) Kloeppner, L. J.; Duran, R. S. *Langmuir* **1988**, *4*, 6734.

(5) Pedrosa, J. M.; Pérez, M.; Prieto, I.; Martín-Romero, M. T.; Möbius, D.; Camacho, L. *Phys. Chem. Chem. Phys.* **2002**, 2329.

(6) Huo, Q.; Russell, K. C.; Leblanc, R. M. *Langmuir* **1998**, *14*, 2174.

(7) Pedrosa, J. M.; Martín-Romero, M. T.; Camacho, L. *J. Phys. Chem. B* **2002**, *106*, 2583.

(8) Tang, X.; Schneider, T. W.; Walker, J. W.; Buttry, D. A. *Langmuir* **1996**, *12*, 5921.

(9) Fernández, A. J.; Martín, M. T.; Ruiz, J. J.; Muñoz, E.; Camacho, L. *J. Phys. Chem. B* **1998**, *102*, 6799.

(10) Cea, P.; Lafuente, C.; Urieta, J. S.; López, M. C.; Royo, F. M. *Langmuir* **1998**, *14*, 7306.

(11) Fernández, A.; Innocenti, M.; Guidelli, R. *J. Electroanal. Chem.* **2002**, *532*, 237.

(12) John, S. A.; Kasahara, H.; Okajima, T.; Tokuda, K.; Ohsaka, T. *J. Electroanal. Chem.* **1997**, *436*, 267.

(13) Marchioni, F.; Venturi, M.; Credi, A.; Balzani, V.; Belohradsky, M.; Elizarov, A. M.; Tseng, H. R.; Stoddart, J. F. *J. Am. Chem. Soc.* **2004**, *126*, 568.

(14) Hiley, S. L.; Buttry, D. A. *Colloid Surf., A* **1994**, 129.

(15) Sagara, T.; Tsuruta, H.; Nakashima, N. *J. Electroanal. Chem.* **2001**, *500*, 255.

(16) Martín, S.; Cea, P.; Gascón, I.; López, M. C.; Royo, F. M. *J. Electrochem. Soc.* **2002**, *149*, E402.

(17) Martín, S.; Haro, M.; Villares, A.; López, M. C.; Cea, P. *J. Electroanal. Chem.* **2005**.

(18) Martín, S.; Cea, P.; Lafuente, C.; Royo, F. M.; López, M. C. *Surf. Sci.* **2004**, *563*, 27.

(19) Obeng, Y. S.; Founta, A.; Bard, A. J. *New J. Chem.* **1992**, *16*, 121.

(20) Fernández, A. J.; Ruiz, J. J.; Camacho, L.; Martín, M. T.; Muñoz, E. *J. Phys. Chem. B* **2000**, *104*, 5573.

(21) Yamada, H.; Imahori, H.; Nishimura, Y.; Yamazaki, I.; Ahn, T. K.; Kim, S. K.; Kim, D.; Fukuzumi, S. *J. Am. Chem. Soc.* **2003**, *125*, 9129.

(22) Fernandes Diniz, J. M. B.; Armitage, D. A.; Linford, R. G.; Pavlidis, V. H. *Langmuir* **1992**, *8*, 2084.

(23) Ferro, S.; De Batisti, A. *J. Phys. Chem. B* **2003**, *107*, 7567.

(24) Raymo, F. M.; Alvarado, R. J.; Pacsial, E. J.; Alexander, D. *J. Phys. Chem. B* **2004**, *108*, 8622.

(25) Summers, L. A. *The Bipyridilium Herbicides*; Academic Press: New York, 1980.

(26) Qian, D. J.; Nakamura, C.; Miyake, J. *Thin Solid Films* **2000**, *374*, 125.

(27) Haiss, W.; van Zalinge, H.; Höbenreich, H.; Bethell, D.; Schiffrin, D. J.; Higgins, S. J.; Nichols, R. J. *Langmuir* **2004**, *20*, 7694.

(28) Lozano, P.; Fernández, A. J.; Ruiz, J. J.; Camacho, L.; Martín, M. T.; Muñoz, E. *J. Phys. Chem. B* **2002**, *106*, 6507.

(29) Monk, P. M. S. *The viologens. Physicochemical properties, synthesis and applications of the salts of 4, 4′-bipyridine*; Wiley: New York, 1998.

(30) Rembaum, A.; Hadek, V.; Yen, S. P. S. *J. Am. Chem. Soc.* **1971**, *93*, 2532.

(31) Ashwell, G. J. *Phys. Status Solidi B* **1978**, *86*, 705.

(32) Ashwell, G. J.; Allen, J. G.; Cross, G. H.; Nowell, I. W. *Phys. Status Solidi A* **1983**, *79*, 455.

(33) Ashwell, G. J.; Allen, J. G.; Goodings, E. P.; Nowell, I. W. *Phys. Status Solidi A* **1984**, *82*, 301.

(34) Houghton, T. J.; Wallwork, S. C. *J. Chem. Res., Synop.* **1999**, *3*, 196.

(35) Kuhn, H.; Möbius, D.; Bücher, H. Spectroscopy of Monolayer Assemblies. In *Techniques of Chemistry*; Weissberger, A., Rossiter, B. W., Eds.; Wiley: New York, 1972; Vol. I, Part IIIB.

(36) Mertesdorf, C.; Ringsdorf, H. *Liq. Cryst.* **1989**, *5*, 1757.

(37) Scoberg, D. J.; Furlong, D. N.; Drummond, C. J.; Grieser, F.; Davy, J.; Prager, R. H. *Colloid Surf.* **1991**, *58*, 409.

(38) Hui, S. W.; Yu, H. *Langmuir* **1992**, *8*, 2724.

(39) McFate, C.; Ward, D.; Olmsted, J. I. *Langmuir* **1993**, *9*, 1036.

(40) Helmholtz, H. *Abh. Thermod.* **1902**, *51*.

(41) Davies, J. T. *Proc. R. Soc. London* **1951**, *A208*, 224.

(42) Davies, J. T. *J. Colloid Sci.* **1956**, *11*, 377.

(43) Davies, J. T.; Rideal, E. K. *Interfacial Phenomena*; Academic Press: New York, 1993.

(44) Shapovalov, V.; Tronin, A. *Langmuir* **1997**, *13*, 4870.

(45) Padma, P.; Kumar, T. V.; Singh, T. C. *Proc. Indian Acad. Sci.* **1995**, *107*, 67.

(46) Kuhn, H.; Försterling, H. D. *Principles of Physical Chemistry*; John Wiley & Sons: New York, 1999.

(47) Silverstein, R. M.; Clayton Bassler, G.; Morril, T. C. *Spectrometric Identification of Organic Compounds*, 5th ed.; John Wiley & Sons, Inc.: New York, 1991.

(48) Gil, A.; Arístegui, I.; Suárez, A.; Sández, I.; Möbius, D. *Langmuir* **2002**, *8*, 8527.

(49) He, W.; Vollhardt, D.; Rudert, R.; Zhu, L.; Li, J. *Langmuir* **2003**, *19*, 385.

(50) Zhang, Y.; Tun, Z.; Ritcey, A. M. *Langmuir* **2004**, *20*.

(51) Xiao, Y.; Ritcey, A. M. *Langmuir* **2000**, *16*, 4252.